The application of response surface methodology and Design-Expert® for analysis of ciprofloxacin removal from aqueous solution using raw rice husk: kinetic and isotherm studies

Husham AbdMunaf Atta*, Khalid Khazzal Hummadi, Mohanad J. M-Ridha

College of Engineering, University of Baghdad, 17635 Baghdad, Jadiriya, Iraq, emails: husham@uobaghdad.edu.iq (H. AbdMunaf Atta), dr.khalid.hummadi@coeng.uobaghdad.edu.iq (K.K. Hummadi), muhannadenviro@coeng.uobaghdad.edu.iq (M.J. M-Ridha)

ABSTRACT

Antibiotics are critical pollutants that have a major threat to human health and have been reported in many water sources worldwide. The present study reports the usage of raw rice husk (RRH) that is capable of adsorbing ciprofloxacin (CPX) from aqueous solution. Response surface methodology (RSM) was applied to optimize the sorption process. Four adsorption variables (pH, Time, initial concentrations and adsorbent dosage) were investig ated and a quadratic model was developed for the CPX removal percentage. The low prediction error of 1.963 indicates the high prognostic ability of RSM. High regression coefficient (R^2 = 0.9910) and the predicted (R^2 of 0.9521) is in acceptable agreement with the adjusted (R^2 of 0.9826); that is, the difference is less than 0.2, which supports the model significance. Batch experiments were also analyzed to understand the process isothermal, thermodynamic and kinetic characteristics. Characterization of RRH was done using scanning electron microscopy and Fourier-transform infrared spectroscopy and point of zero charge. The results showed that the process followed Langmuir isotherm and Elovich kinetics. The thermodynamic coefficients suggested that the adsorption process was endothermic and spontaneous in nature.

Keywords: Ciprofloxacin; Raw rice husk adsorbent; Adsorption isotherm; Kinetic models; Optimization

1. Introduction

Antibiotics are extensively used to treat infectious diseases in humans and animals. It is representing 11% of the world's total applied medicines. Antibiotics are not completely metabolized in the body; resulting the extraction of these compounds to the environment [1]. Antibiotics presence in water streams represent a serious environmental challenges since these antibiotics are difficult to remove and gradually accumulate in living organisms [2]. Wastewater treatment plants effluents, pharmaceuticals manufacturing plants, aquaculture and animal husbandry are different channels for antibiotics to enter into the aquatic environment [3]. When native organisms interact with antibiotics, this could change their microbial genetics and the community structure, and when the ecosystem is in a continuous exposure to antibiotics, this can promote the selection of resistant bacterial strains, which include potential pathogens [4]. Biosorption process, which means the employment of biomass in the removal of antibiotics from aqueous solution has been considered the most promising alternative method in replacing traditional methods like precipitation, electro-dialysis, membrane filtration, and reversed osmosis in removing different contaminants [5,6].

Adsorption is a low cost method with high efficiency, easy to operate, flexible and with much less sludge disposal

* Corresponding author.

problems [6]. Solution characteristics such as the pKa of the adsorbate, adsorbent point of zero charge (pH_{PZC}) and pH highly influence the adsorption process [7].

The adsorption process consist of several stages; at first the solute transports in the bulk of the solution (convection) and the disperse through the interstices of the sorbent, then it transports across the liquid thin film surrounding sorbent particles; followed by the solute diffusion in the quiescent liquid contained in the sorbate particle pores and along the pore walls; and finally the surface diffusion of the solute molecules on the sorbent surface. Adsorption overall rate could be controlled by any of these stages; or a combined effects of a few of them [8]. Various biosorbents have been used to remove antibiotics from aqueous solutions, such as corncobs for sulfamethoxazole removal [9], maize stalks for tetracycline removal [10], *Calotropis procera* for ciprofloxacin, and norfloxacin removal [11].

In order to study the relationships among the independent variables that have been selected in this study (pH, initial concentration, biosorbent dosage and time) and the removal efficiency as a single response, experimental statistical design is considered as one of most useful methods to provide statistically significant models of a certain phenomenon by employing the minimum number of calculated experiments [12–14]. It's also can be used to evaluate the interactions among the variables and can be used for the multivariable process optimization. Response surface methodology (RSM) and central composite design (CCD) were used for the modeling and analysis of problems in which a response of interest is influenced by several variables to optimize the same response [6,15,16]. The second-order (quadratic) model was used to determine the mathematical model and it is shown in Fig. 1.

Ciprofloxacin is one of the quinolones antibiotics; it is a toxic organic substance that is hazardous to the environment. It can interfere with the photosynthesis pathway of plants, leading to abnormal plant morphologies and geno-toxicity [17]. Ciprofloxacin (CPX) is highly soluble in aqueous solutions under various pH conditions [8], and it was detected in the samples of raw and finished water of two Iraqi water treatment plants with maximum concentration of 1.270 µg/L [18].
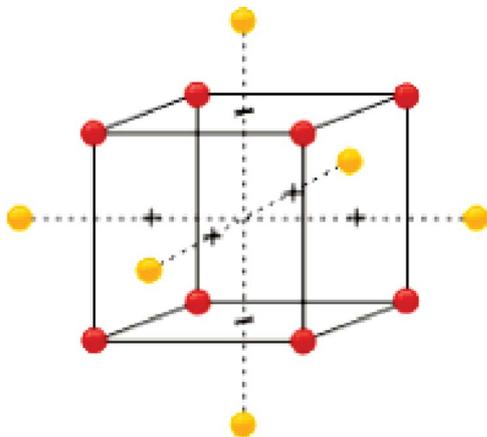
Some adsorbents have been used to treat CPX polluted water, such as magnetic N-doped porous carbon [19], cube-shaped nano-MgO [20], bentonite [8], clinoptilolite [21], MWCNT [22], montmorillonite, alumina and activated carbon [23]. Due to the cost of some adsorbates there is an urgent need to find inexpensive, environmentally friendly and high availability materials. A growing interest on agro-industrial waste to treat different pollutants has been recognized recently. Rice husk (RH), which is considered a waste biomass material, recently considered as an effective and low-cost alternative biosorbent for environmental pollutants [24]. Rice husk has been effective in removing different pollutants, including beta-lactam cefixime [25], tetracycline [26], dyes [27,28] and heavy metals [29,30]. Some researchers have chemically and physically modified RH to optimize their adsorbent capacity which unfortunately increases the cost of the adsorbent [31]. Considering the fact that no study has been done on the adsorption of CPX from aqueous solution by raw rice husk, this study objective is to investigate the modeling and optimization of ciprofloxacin adsorption from aqueous solution by raw rice husk (RRH) without any modifications and in cost effective method under different experimental conditions, by using response surface methodology based on central composite design and study the kinetics, adsorption isotherms models and thermodynamic of the adsorption process.

2. Materials and methods

2.1. Ciprofloxacin stock solution preparation

Ciprofloxacin, has the empirical formula of ($C_{17}H_{18}FN_3O_3$), its molecular weight is 331.41 and the chemical name is 1-cyclopropyl-6-fluoro-1, 4-dihydro-4-oxo-7-(1-piperazinyl)-3-quinolinecarboxylic acid, shown in Fig. 2. [32]

Stock CPX solution was prepared by dissolving 500 mg of CPX in 1 L of distilled water. Experimental solutions of different concentrations were prepared by diluting the stock solution. For adjusting the pH, HCl and NaOH of 0.1 N solutions (Sigma-Aldrich) were used. All the glassware used were washed and rinsed several times with deionized water.

2.2. Adsorbent preparation

In this study, raw rice husk was used as a low cost natural agricultural waste. Raw rice husk was collected from Al-Mishkhab – Najaf-Iraq rice mills. RRH was washed with deionized water (DI) several times to remove the dirt and impurities, and then air-dried for 24 h. The air dried RRH was sieved through a 2–1 mm mesh sieves to obtain a uniform size and kept in an enclosed container.

2.3. Adsorbent characterization

The microstructure of the RRH was observed by scanning electron microscopy (SEM) (Tescan Vega II-Czech Republic). Fourier-transform infrared spectroscopy (IRAffinity-1, Shimadzu, Japan) absorption spectrums using the potassium bromide disc method for the adsorbent pre and post adsorption were performed. Point of zero charge for the RRH was calculated using salt addition method.
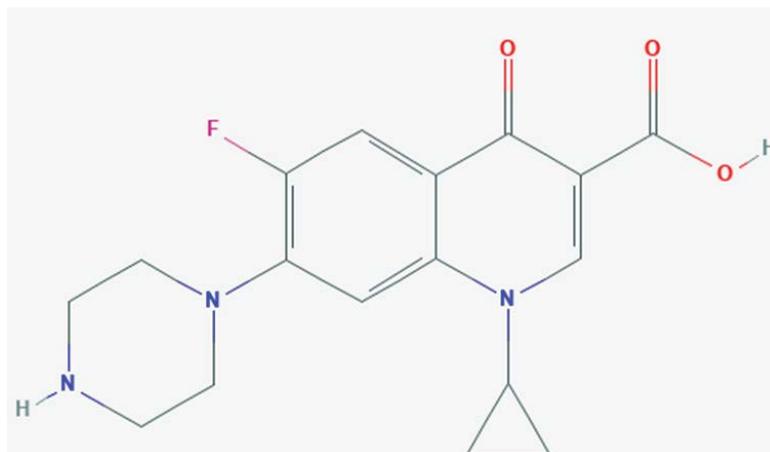

Fig. 1. CCD of four parameters, dimensional concept.

Fig. 2. Ciprofloxacin chemical structure.

2.4. Instrumentation

The pH measurements were performed using the hatch pH-meter (Czech Republic). A DR-5000 Hach UV/Visible spectrophotometer was used to measure the absorbance spectra for CPX in the wavelength range of 190–1,100 nm. The samples were agitated in the shaker at 150 rpm for a determined time to reduce the surface mass transfer resistance in the separation phase.

2.5. Adsorption experiment

One hundred ml of ciprofloxacin solution of different initial concentrations 5–100 mg/L was prepared in 250 mL Erlenmeyer flasks, to which rice husk loading in range of 0.5–3 g/100 mL was added with various pH values 2–8 and the samples were agitated in a shaker at 150 rpm for determined time 5–180 min. After agitation, the samples were analyzed to determine the CPX residuals using Hatch DR-5000 UV-VIS Spectrophotometer. Each run was performed in duplicate, and the mean values were used as the removal efficiency response.

The removal efficiency was calculated by the following equation [33]:

$$R = \frac{(C_0 - C_e)}{C_0} \times 100\% \tag{1}$$

2.6. Design of experiments

The design of experiment was carried out using Design-Expert software version 12 (Stat-Ease, Inc., Minneapolis, MN 55413, USA). Four factors were considered in the study pH, time, initial concentration and rice husk weight during the design process. Different stock solutions were prepared according to the variables details that were given by the design of experiment for each run as shown in Table 1, with one response which is the mean removal percentage of ciprofloxacin.

Quadratic model was used with RSM/CCD was applied to determine the coefficients in a second-order polynomial mathematical mode to study the ciprofloxacin removal under different parameters. The number of experiments was calculated according to Eq. (2):

$$N = 2^k + 2k + n_c \tag{2}$$

where N is number of experiments; k is the number of variables and n_c is the number of central points [34].

Eq. (3) expresses the quadratic model which was developed for the adsorption of the ciprofloxacin.

$$y = \beta_0 + \sum_{i=1}^{4} \beta_i x_i + \sum_{i=1}^{4} \sum_{j=1}^{4} \beta_{ij} x_i x_j + \sum_{i=1}^{4} \beta_{ii} x_i^2 + \varepsilon \tag{3}$$

where y is the response (removal percentage); β_0, β_i, β_{ii} are the intercept, linear, quadratic and interaction regression coefficients of variables, respectively; x_i and x_j are the independent variables while ε is the residual term [35].

3. Results and discussion

3.1. Characterization of absorbent

Fourier-transform infrared spectroscopy (FTIR) analysis offers excellent information on the nature of the RRH surface functional groups. Different chemical functional groups have been identified as potential adsorption sites to be responsible for binding antibiotics.

The FTIR of RRH before and after adsorption of ciprofloxacin is shown in Fig. 3.

The wide peak at 3,242.34 in RRH and 3,221 cm^{-1} in CPX-RH is representing the hydroxyl functional groups O–H [36]. The peak at 2,914 cm^{-1} indicates the C–H stretching vibration of alkyl functional groups and this peak was changed to 2,883 cm^{-1} [37]. The 1,643 and 1,438 cm^{-1} peaks at the unloaded RRH and 1,653 and 1,514 cm^{-1} of CPX loaded RH represent the presence of carbonyl (C=O) group [38]. The peak at 1,062.78 in RRH and 1,086 cm^{-1} in CPX loaded RH is mainly attributed to the carboxylic acids and alcohols (C–O) [39]. The peak at 640 and 460 cm^{-1} in RRH and 634 and 465 in CPX-RH is probably for the presence of aromatic compounds in RH [36]. The FTIR results showed the presence of various functional groups ON RRH before and after
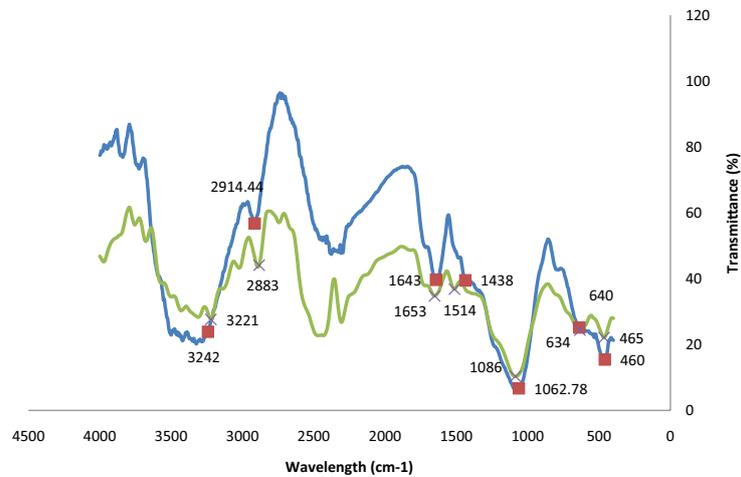
Fig. 3. IR spectrum of RRH (blue line) and RH-CPX (green line) samples.

the sorption of CPX. Some FTIR peaks were disappeared shifted and some new peaks were emerged. In the sorption of CPX on RH mainly aliphatic C–H groups, hydroxyl (–OH), carboxylic (C–O) and aromatic compounds functional groups on the surface of rice husk play the major role in biosorption of CPX.

SEM images are shown in Fig. 4. These images reveal that RRH had a coarse, highly porous surface, and it consists of several non-uniforms and separated aggregates. Moreover, there are many long grooves and big ravines in the outer surface of RRH. The morphological properties of

the RRH surface represent a positive point, as they are providing a high surface area and active sites for adsorbing the antibiotics molecules. On comparing the SEM image of RRH and RH-CPX, it can be noticed that the morphological properties of RRH are significantly altered during the process of antibiotic adsorption. Furthermore, the surface of RH becomes smoother, and some previously separated aggregates are enclosed which might be a result of adsorption of the antibiotics on active sites of the RH.

The point of zero charge (pH_{PZC}) is an important analysis to characterize adsorbents. RRH point of zero charge
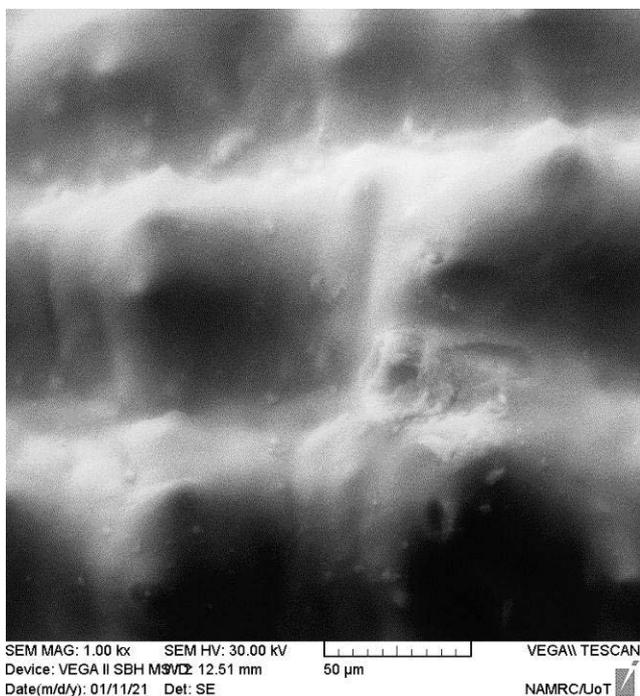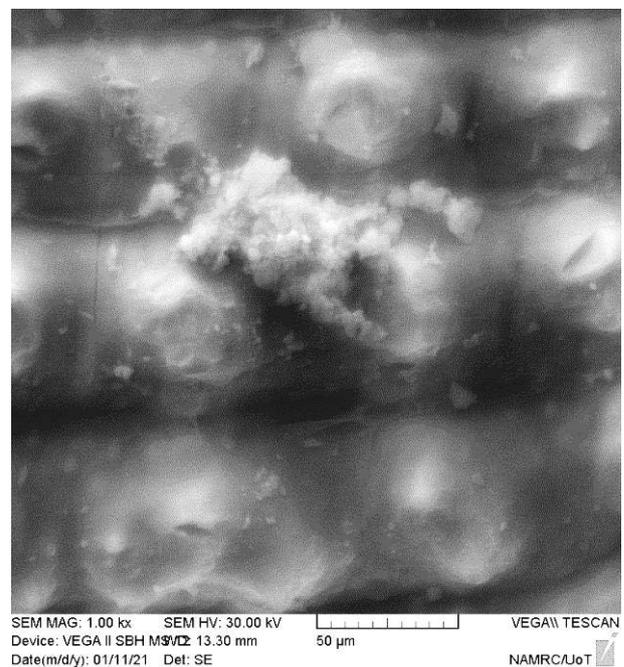
Fig. 4. SEM for RRH and RH-CPX.

of was calculated by using the salt addition method [6]. Conical flasks with 250 mL capacity were filled with 100 mL of 0.1 mol/L NaCl solution. Solution pH ranged between 2 and 8 with HCl or NaOH addition. RH of 1 g weight was added to different conical flasks and shake for 24 h. Initial and final solutions pH was calculated and their difference was recoded. As shown in Fig. 5, the pH_{PZC} represents the value that the curve intersects the zero change value axis (ΔpH vs. $pH_{initial}$) and from the figure the pH_{PZC} was 6.8.

3.2. Model validation and diagnostic analysis

The adsorption analysis using RRH which was done on aqueous ciprofloxacin solution with applying RSM/CCD is shown in Table 1, which shows the variables setting and the actual and predicted results. The design consists of 30 experiments, including several replicate experiments to check the consistency of the adsorption process. The small relative standard deviation (1.61%) shown in Table 2 is

an evidence of the model consistency. Moreover, a higher regression coefficient ($R^2 = 0.9910$) and the predicted R^2 of 0.9521 is in acceptable agreement with the adjusted R^2 of 0.9826; that is, the difference is less than 0.2 which supports the model significance [40]. The high R^2 values means that there is a good fit between the experimental and predicted values [41]. The model has a low coefficient of variance value (3.17) which indicates the high reliability of the model. Adeq. precision measures the signal to noise ratio

Table 2
Statistical information of the model

Std. Dev.	1.61	R^2	0.9910
Mean	50.92	Adjusted R^2	0.9826
C.V. %	3.17	Predicted R^2	0.9521
		Adeq. precision	40.9233

Table 1
The criteria for each parameter used in the experiments as designed by Design-Expert v12 using RSM/CCD

| Run	Factor 1	Factor 2	Factor 3	Factor 4	Response	Predicted
	A: pH	B: Time	C: Concentration	D: Dosage	R1	value
1	5	92.5	52.5	3	66.98	65.48
2	6.5	48.75	76.25	1.125	67.98	22.65
3	3.5	48.75	76.25	1.125	68.98	25.35
4	5	92.5	52.5	1.75	69.98	53.33
5	3.5	136.25	76.25	2.375	70.98	58.15
6	3.5	48.75	28.75	1.125	71.98	49.33
7	3.5	136.25	76.25	1.125	72.98	37.17
8	3.5	48.75	28.75	2.375	73.98	57.61
9	6.5	48.75	76.25	2.375	74.98	50.4
10	5	92.5	52.5	1.75	75.98	53.33
11	3.5	48.75	76.25	2.375	76.98	50.96
12	6.5	136.25	76.25	2.375	56.59	56.98
13	5	92.5	52.5	1.75	52.71	53.33
14	5	92.5	100	1.75	35.17	35.85
15	6.5	48.75	28.75	1.125	45.86	46.46
16	6.5	136.25	28.75	1.125	59.15	60.71
17	5	5	52.5	1.75	42.61	41.56
18	6.5	136.25	76.25	1.125	33.75	33.87
19	6.5	48.75	28.75	2.375	55.25	56.89
20	3.5	136.25	28.75	2.375	66.86	67.81
21	5	92.5	52.5	1.75	55.09	53.33
22	8	92.5	52.5	1.75	46.07	44.59
23	2	92.5	52.5	1.75	49.79	48.62
24	5	180	52.5	1.75	64.58	62.98
25	5	92.5	52.5	0.5	35.24	34.09
26	5	92.5	52.5	1.75	52.99	53.33
27	3.5	136.25	28.75	1.125	62.76	64.17
28	6.5	136.25	28.75	2.375	65.48	66.49
29	5	92.5	52.5	1.75	53.31	53.33
30	5	92.5	5	1.75	72.65	69.33
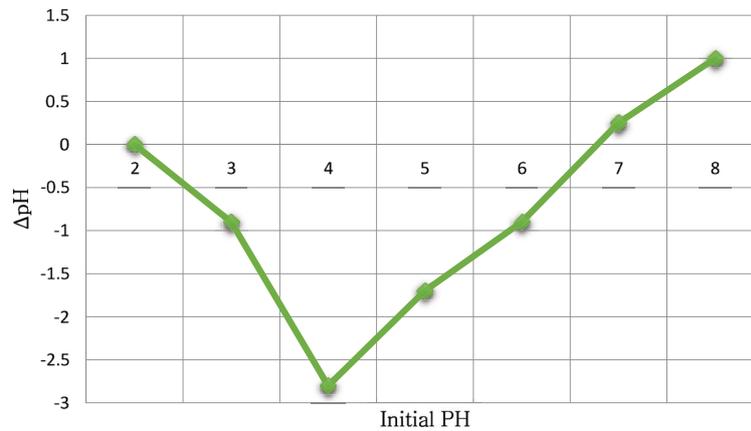
Fig. 5. Estimation of point of zero charge.

in which, greater than four ratios is desirable. The study ratio was 40.923 which indicate an adequate signal and the model can be used within the proposed design. The RSM/CCD batch method is therefore capable of providing consistent results and it is suitable to be used in the investigation of the adsorption of CPX onto raw rice husk.

Table 3 describes the ANOVA for the quadratic model for CPX percentage removal, showing mean squares, df, sum of squares, F-value and Prob. > F values of each factor.

ANOVA validates the importance and how adequate the model was. The transformation model has a very small p-value < (0.0001) (p-values less than 0.05 show that the model is significant at a 95% confidence limit) [41,42] and large value of F (117.99) which indicate the statistical significance of the model was [40].

Lack of fit F-values was found as 4.49 implying that the lack of fit is not significant relative to the pure error for the model.

The model equation for ciprofloxacin removal efficiency is:

$$
\begin{aligned}
R =\ &+34.82200 + 5.95400 \times pH + 0.271828 \times Time - 0.766970 \\
&\times Concentration + 6.24368 \times Dosage - 0.002286 \times pH \\
&\times Time + 0.001123 \times pH \times Concentration + 0.570667 \\
&\times pH \times Dosage - 0.000727 \times Time \times Concentration \\
&- 0.042423 \times Time \times Dosage + 0.291874 \times Concentration \\
&\times Dosage - 0.747130 \times pH^2 - 0.000138 \times Time^2 - 0.000330 \\
&\times Concentration^2 - 2.26827 \times Dosage^2.
\end{aligned}
\tag{4}
$$

Fig. 6 shows the predicted values vs. the experimental values for CPX removal, portraying that the developed models successfully captured the relation between the adsorption process variables to the responses.

3.3. Model interpretation

Three dimensional (3D) models were used to graphically present the model variables in space to visualize and evaluate the effect of the variables on the response factor.

3.3.1. Effect of initial pH

CPX have three species, zwitterion species around neutral pH 6.9–8.9, cationic species at lower pH (below 6.8), and anionic species at higher pH values (higher than 8.8) [43,44].

When the initial pH was less than 5 (pH < pK_{a1}), the adsorption of CPX onto RH decreased with decreasing pH (Figs. 7C and 8). This might be a result of the increasing electrostatic repulsion between the amine groups on CPX molecules and the positive charge on the RRH [24]. Meanwhile, increasing the initial pH leads to increase CPX removal which might be resulted from the relatively low protonation of functional groups on the surfaces, which competed with the polar attraction of CPX in the aqueous solution. Removal efficiency varied slightly in the pH range of 5–8, probably because the RH presented strong buffering effect to solution pH that could be resulted from its higher silicon contents (surface silicon hydroxyls) [45,24]. Researchers found that optimum pH for fluoroquinolone antibiotics on positive charge adsorbents was between 5 and 6 [46–49]. Other researchers found that the best RH adsorption removal for positive pollutants was at the same range [36,37,50,51] Removed CPX using RH that have PZC of 7.5 with optimum pH of 6 and the q_{max} was 2.33 mg/g.

3.3.2. Effect of rice husk dosage

The adsorbent dosage significantly influences the adsorption process as it influences the net charge amount and the total specific surface area [52]. The removal efficiency increased significantly when the RH dosage increased from 5 to 30 g/L as shown in Figs. 7C, E, F and 9. The increment in removal efficiency with increasing RH dose is probably a result of the increased pore volume, greater surface area and unsaturated sites available on RH surface at higher doses [53], providing more functional groups and active adsorption sites that lead to higher removable percentages [52].

3.3.3. Effect of time and initial concentration

The contact time is an important factor which crucially affects the adsorption process. Contact time can

Table 3
ANOVA for the quadratic model

| Source	Sum of squares	df	Mean square	F-value	p-value	
Model	4,298.14	14	307.01	117.99	<0.0001	significant
A-pH	14.32	1	14.32	5.50	0.0332	
B-time	428.63	1	428.63	164.74	<0.0001	
C-concentration	1,015.26	1	1,015.26	390.19	<0.0001	
D-dosage	808.20	1	808.20	310.62	<0.0001	
AB	0.3600	1	0.3600	0.1384	0.7151	
AC	0.0256	1	0.0256	0.0098	0.9223	
AD	4.58	1	4.58	1.76	0.2045	
BC	9.12	1	9.12	3.51	0.0808	
BD	21.53	1	21.53	8.27	0.0115	
CD	300.33	1	300.33	115.43	<0.0001	
A^2	77.51	1	77.51	29.79	<0.0001	
B^2	1.92	1	1.92	0.7391	0.4035	
C^2	0.9493	1	0.9493	0.3649	0.5548	
D^2	21.53	1	21.53	8.28	0.0115	
Residual	39.03	15	2.60			
Lack of fit	35.12	10	3.51	4.49	0.0555	not significant
Pure error	3.91	5	0.7814			
Cor. total	4,337.17	29				
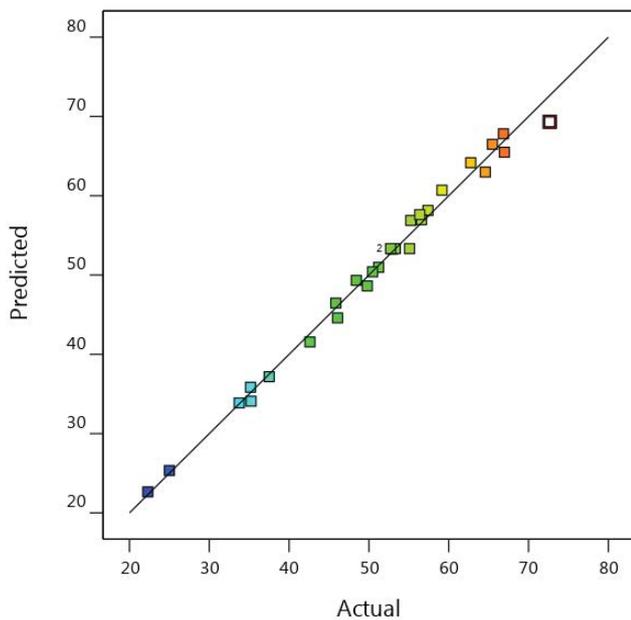
Fig. 6. Predicted vs. actual result.

influence the economic efficiency of the process as well as the adsorption kinetics [54]. CPX removal was increased with increased time as shown in Figs. 7A, D, E and 10. Since the sorbent had abundant binding sites, the gradual occupancy of these sites over different times resulted in an increase in removal of CPX till the equilibrium, the sorption will become constant because the active sites are now saturated so there will be no or minimum adsorption [55].

The removal efficiency decreased as the initial concentration of CPX increased from 5 ppm to 100 ppm as shown in Figs. 7B, D, F and 11.

At lower concentrations, the CPX-RH interaction is greater since the ratio of available active sites to initial CPX concentration is greater, while in higher initial concentration the ratio is lower as result of active site saturation which eventually decreases the removal efficiency [53].

3.3.4. Combined effect of pH, time, concentration and dosage on CPX removal percentage

The 3D plot of the interactive effect of pH, time, initial concentration and RRH dosage on the adsorption of CPX, are presented in Fig. 7A–F and the quadric model Table 3. The removal of the CPX is influenced significantly by the interaction of time and concentration with F value of 115.43 and less with other parameters interactions 0.1384, 0.0098, 1.76, 3.51, 8.27 for pH and time, pH and concentration, pH and dosage, time and concentration and time and dosage respectively. The interaction of parameters confirmed what was mentioned earlier that higher removal percentage occurred with pH near 5, longer time, less CPX concentration and more RRH dosage.

3.3.5. Process optimization

The desirability function is applied to optimize the removal efficiency as a single response, by maximizing it and transforming the values of the obtained responses into values of desirability functions that range between 0 and 1. The value 1 is designated for the ideal performance of the study factors while the zero value is designated for values that do not have a desirable response
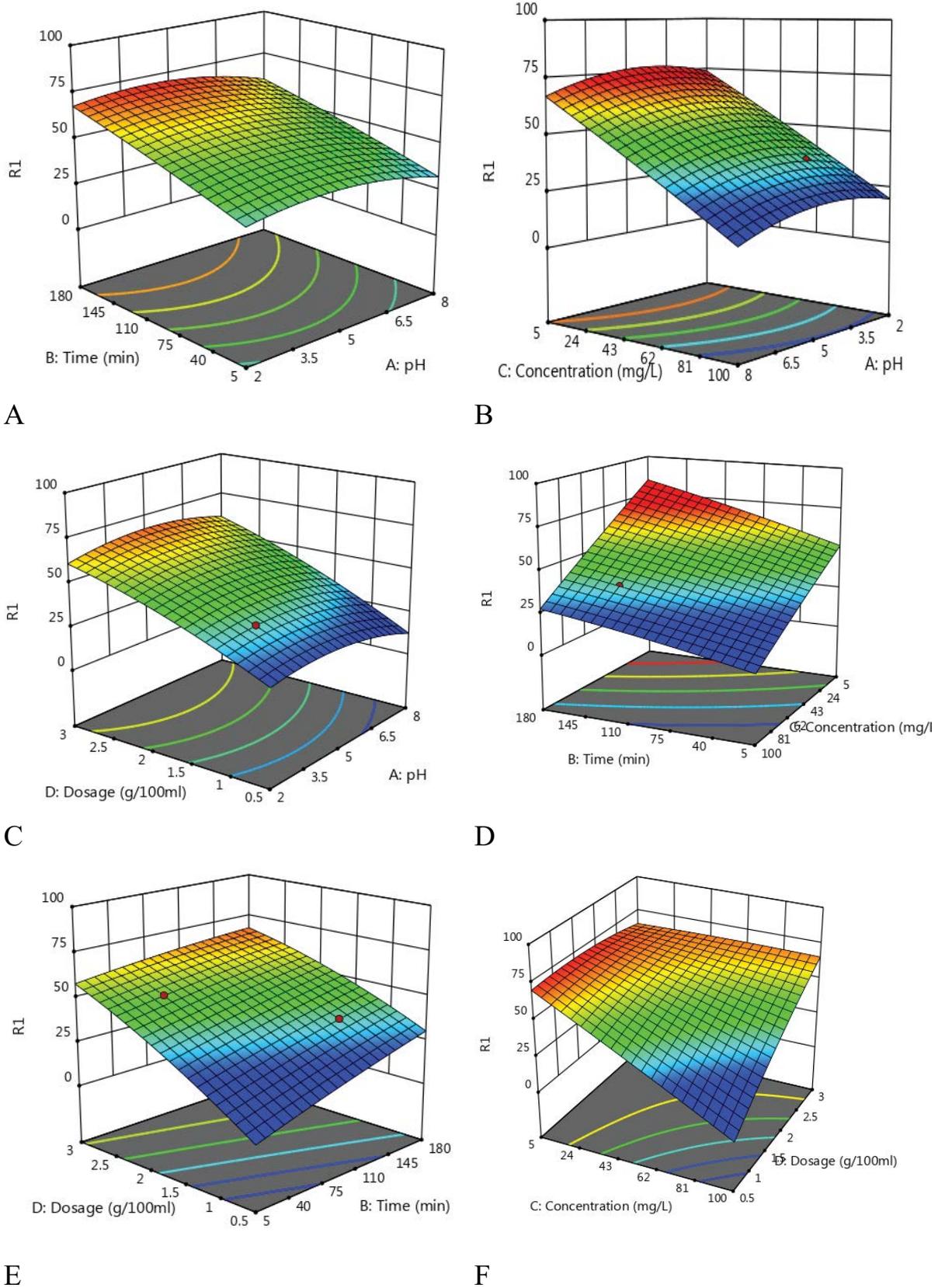
Fig. 7. 3D surface plot representing combined effect of (A) contact and time pH, (B) initial concentration and pH, (C) adsorbent dosage and pH, (D) time and initial concentration, (E) time and adsorbent dosage and (F) adsorbent dosage and initial concentration on the ciprofloxacin removal.
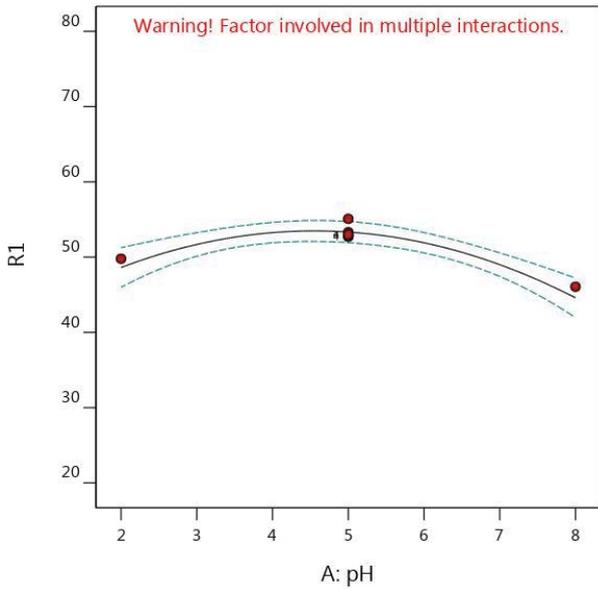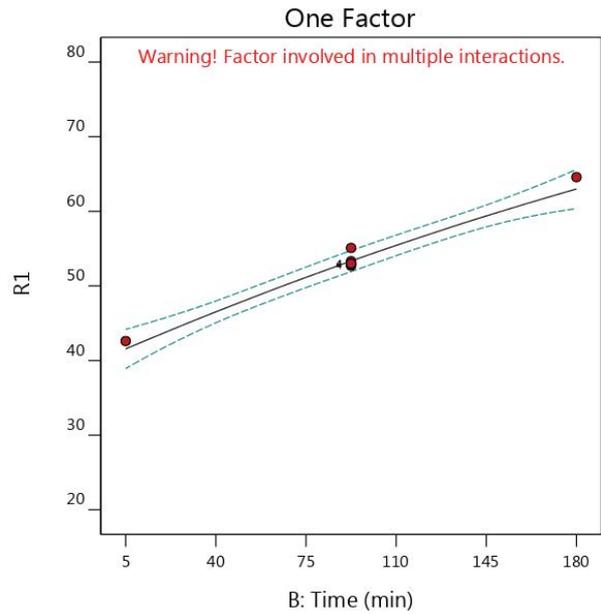
Fig. 8. pH effect on CPX adsorption.

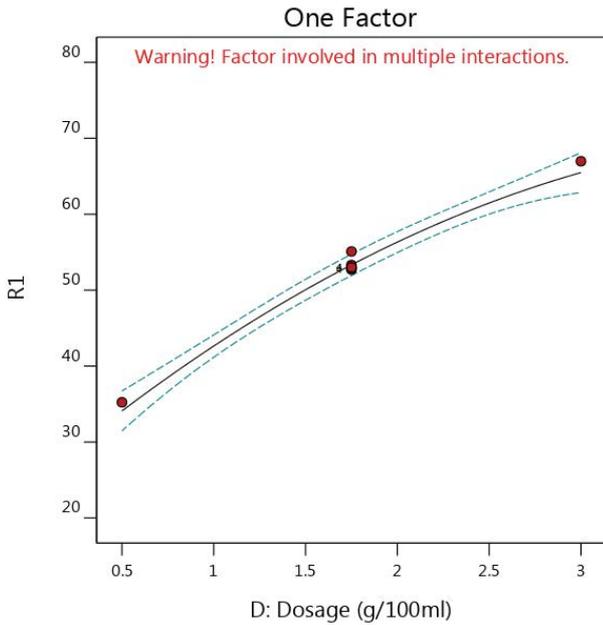Fig. 10. The effect of time on CPX adsorption.
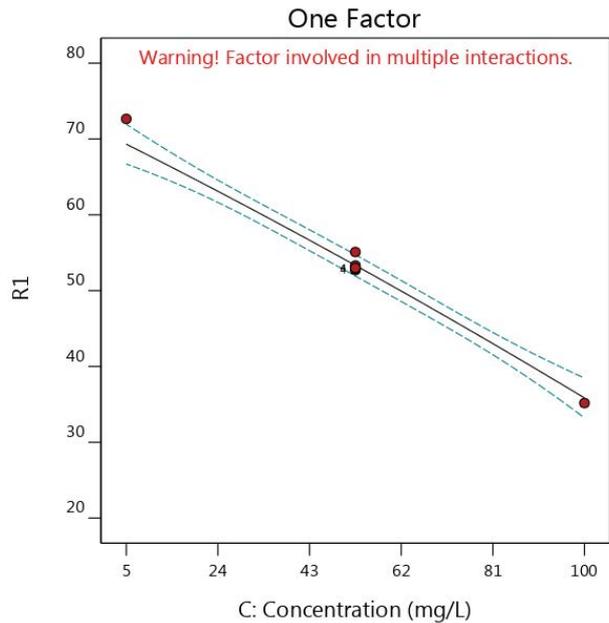

Fig. 9. Dosage effect on CPX adsorption.

Fig. 11. The effect of concentration on CPX adsorption.

[41,42]. This combination of RSM with the desirability function is called. The optimization of CPX adsorption onto RRH was carried out by the function of desirability, using design-expert software (Stat-Ease, Inc., Minneapolis, MN 55413, USA) [56]. The optimization analysis searches for a combination of factor levels that simultaneously satisfy the criteria placed on each of the responses and factors. An optimum setting for the formulation was generated by the numerical optimization technique and the process was optimized for the dependent (response) and the parameters. The optimized formula was reached by setting the response at maximum value and the all the factor were set in range. Fig. 12 shows an optimization solution with desirability of 1, 00, pH = 5.08, time = 152.32 min, concentration = 9.45 mg/L and the dosage = 2.5 g/100 mL. The low % prediction error of 1.963 indicated the high prognostic ability of RSM.

Seven experiments were executed to experimentally check the optimum conditions under the same conditions. The results showed high coefficients of determination (R^2) value of 0.98. The high degree of agreement between the experimental results and the predicted optimum results
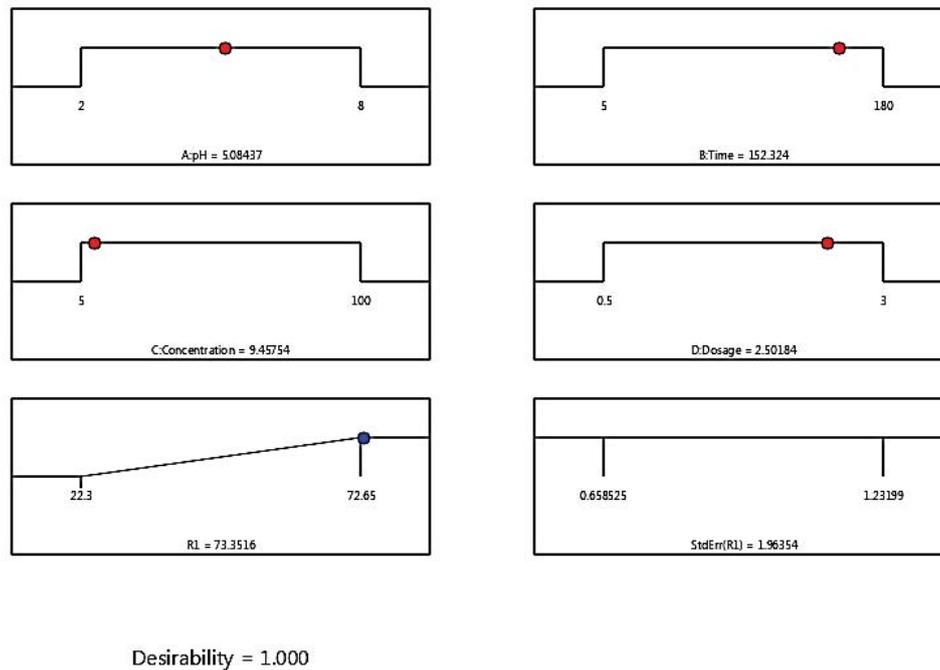
Fig. 12. Optimization solution.

indicate that the CCD could be used effectively for the evaluation and optimization of the removal efficiency of CPX from aqueous solution using raw rice husk (RRH).

3.4. Isotherm models

Isotherm models are very important in studying and designing adsorption system. Four models (Langmuir, Temkin, Brunauer–Emmett–Teller (BET) and Freundlich) were studied for the removal of CPX; the parameters of each model are displayed in Table 5a and Fig. 13. Langmuir model has the best correlation Coefficient (R^2) with 99.5% followed by with Freundlich 99.4%, Temkin 99.3%, and BET 99.2%.These results suggest that the adsorption was not onto a uniform site rather a multilayer adsorption and still the monolayer adsorption plays a great role in the removal process. The monolayer maximum uptake q_{max} is 3.985 mg/g and the n value is larger than 1 indicate that the adsorption is favorable [57]. Table 4 provides a list of researches that used different adsorbents to remove CPX with their adsorption capacity.

3.5. Adsorption kinetic

The results in Table 5b show that high R^2 and low CHI square, sum of the squares of errors (ERRSQ) and average relative error (ARE) values characterized the Elovich model, suggesting that this model describes the kinetics of LEV uptake onto RH. The PFO cannot be used due to its very low R^2. Fig. 14 shows that more than 80% removal of all concentrations were in the first hour, which indicate the rapid adsorption rate of adsorption process. The process reaches the equilibrium at 120 min and after that the removal efficiency fluctuates insignificantly.

3.6. Adsorption thermodynamics

In order to examine the thermodynamic parameters (free energy change, enthalpy change and entropy change) four experiments with different temperatures were carried out (298, 303, 308 and 313 K). From Table 6, negative values of ΔG for CPX sorption at the various temperatures, indicating that the adsorption process was spontaneous

Table 4
Adsorbents reported for the removal of CPX from aqueous solution

Biosorbent	Adsorption capacity (mg/g)	Reference
Biochar from potato stem and leaves	23.36	[58]
Enteromorpha prolifera	21.70	[59]
Humic acid/cellulose	10.87	[60]
Biochar from water hyacinth	2.717	[61]
Groundnut shell	0.600	[62]
ZnO nanoparticles	0.160	[62]

Table 5a
Isotherm models

Isotherm model	Parameters				Sum of the squares of errors (ERRSQ)	Average relative error (ARE)	CHI square
Langmuir	q_{max} 3.985	K 0.885		R^2 0.995	0.39	1.57	0.46
Temkin	K 23.458	B 0.56		R^2 0.993	0.04	0.68	0.06
BET	q_m 2.12	b 257.586	C_s 49.532	R^2 0.992	0.014	0.33	0.019
Freundlich	K 6.11	n 1.13		R^2 0.994	0.21	1.56	0.38

Table 5b
Kinetic models

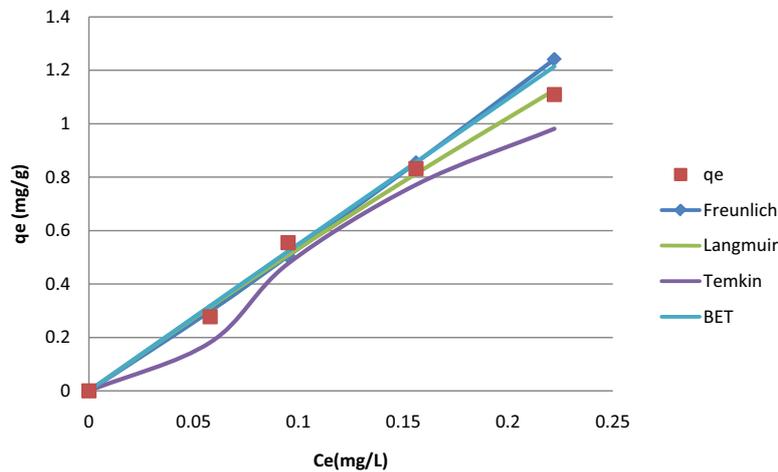| Method	Parameters		R^2	Sum of the squares of errors (ERRSQ)	Average relative error (ARE)	CHI
Pseudo-first-order	K_1 1.689	Q_e 1.030	0.295	0.076	0.914	0.078
Pseudo-second-order	K_2 0.920	Q_e 1.361	0.884	0.125	1.314	0.123
Intraparticle	K_p 0.021	C_i 0.884	0.838	0.017	0.469	0.017
Elovich	α 30.662	β 8.991	0.970	0.113	1.031	0.124

Fig. 13. Isotherm models.

and feasible for the temperatures under investigation [57]. The decreased values of ΔG with the increasing temperature indicate that CPX sorption efficiency was more favorable at higher temperature [63]. Positive ΔH value indicates that the adsorption process is endothermic [64]. The positive value of ΔS confirms the increasing of randomness and disorder of the solid-solute interface at RH surface during the adsorption process [57].

4. Conclusions

In the present study RRH were used in removing CPX from aqueous solutions. RSM and CCD were applied to optimize the sorption process. Four adsorption variables (pH, Time, initial concentrations and adsorbent dosage) were investigated and a quadratic model was developed for the CPX removal percentage. The low % prediction

Table 6
Thermodynamic parameters

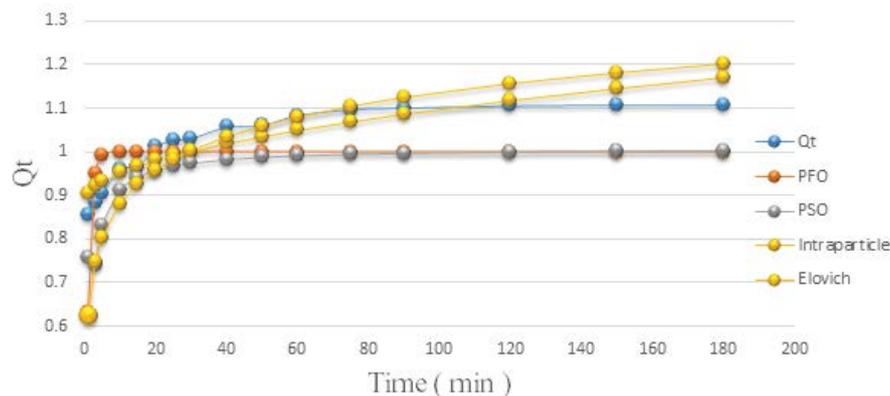| $\Delta H°$ (kJ/mol)	$\Delta S°$ (J/mol K)	$\Delta G°$ (kJ/mol)			
		298	303	308	313
34.40534	119.2035	−927.883	−1,542.6	−2,440.71	−3,220.41

Fig. 14. Kinetic models.

error of 1.963 indicated the high prognostic ability of RSM. High regression coefficient (R^2 = 0.9910) and the predicted R^2 of 0.9521 is in acceptable agreement with the adjusted R^2 of 0.9826; that is, the difference is less than 0.2, which supports the model significance. The adsorption process were found to be following the Langmuir isotherm model emphasizing on the single layer CPX adsorption. The negative Gibb's free energy and positive entropy value indicated that the process is endothermic and spontaneously with increased randomness. The process was best fit to Elovich kinetics model. Hence, it can be concluded that RRH used in this study was an eco-friendly and inexpensive adsorbent.

References

[1] M. Malakootian. K. Kannan, M. Amiri Gharaghani, A. Dehdarirad, A. Nasiri, Y.D. Shahamat, H. Mahdizadeh, Removal of metronidazole from wastewater by Fe/charcoal micro electrolysis fluidized bed reactor, J. Environ. Chem. Eng., 7 (2019) 103457, doi: 10.1016/j.jece.2019.103457.

[2] G. Liu, Z. Zhu, Y. Yang, Y. Sun, F. Yu, J. Ma, Sorption behavior and mechanism of hydrophilic organic chemicals to virgin and aged microplastics in freshwater and seawater, Environ. Pollut., 246 (2019) 26–33.

[3] A.C. Singer, H. Shaw, V. Rhodes, A. Hart, Review of antimicrobial resistance in the environment and its relevance to environmental regulators, Front. Microbiol., 7 (2016) 1–22, doi: 10.3389/fmicb.2016.01728.

[4] M.C. Danner, A. Robertson, V. Behrends, J. Reiss, Antibiotic pollution in surface fresh waters: occurrence and effects, Sci. Total Environ., 664 (2019) 793–804.

[5] Z.N. Garba, I. Bello, A. Galadima, A.Y. Lawal, Optimization of adsorption conditions using central composite design for the removal of copper(II) and lead(II) by defatted papaya seed, Karbala Int. J. Mod. Sci., 2 (2016) 20–28.

[6] B. Zhang, X. Han, P. Gu, S. Fang, J. Bai, Response surface methodology approach for optimization of ciprofloxacin

[7] X. Peng, F. Hu, F.L.Y. Lam, Y. Wang, Z. Liu, H. Dai, Adsorption behavior and mechanisms of ciprofloxacin from aqueous solution by ordered mesoporous carbon and bamboo-based carbon, J. Colloid Interface Sci., 460 (2015) 349–360.

[8] N. Genç E.C. Dogan, Adsorption kinetics of the antibiotic ciprofloxacin on bentonite, activated carbon, zeolite, and pumice, Desal. Water Treat., 53 (2015) 785–793.

[9] M.E. Peñafiel, J.M. Matesanz, E. Vanegas, D. Bermejo, M.P. Ormad, Corncobs as a potentially low-cost biosorbent for sulfamethoxazole removal from aqueous solution, Sep. Sci. Technol., 55 (2020) 3060–3071.

[10] D. Balarak, F. Mostafapour, H. Azarpira, Adsorption kinetics and equilibrium of ciprofloxacin from aqueous solutions using *Corylus avellana* (Hazelnut) activated carbon, Br. J. Pharm. Res., 13 (2016) 1–14.

[11] W. Duan, W. Xiao, N. Wang, B. Niu, Y. Zheng, Removal of three fluoroquinolone antibiotics by NaClO2-modified biosorbent from fruit fiber of *C. Procera*, J. Nat. Fibers, 17 (2020) 1594–1604.

[12] M.O. Saeed, K. Azizli, M.H. Isa, M.J.K. Bashir, Application of CCD in RSM to obtain optimize treatment of POME using Fenton oxidation process, J. Water Process Eng., 8 (2015) e7–e16.

[13] J. Sharma, Sukriti, P. Anand, V. Pruthi, A.S. Chaddha, J. Bhatia, B.S. Kaith, RSM-CCD optimized adsorbent for the sequestration of carcinogenic rhodamine-B: kinetics and equilibrium studies, Mater. Chem. Phys., 196 (2017) 270–283.

[14] V. Alimohammadi, M. Sedighi, Reduction of TDS in water by using magnetic multiwalled carbon nanotubes and optimizing with response surface methodology, J. Environ. Eng., 144 (2018) 04017114, doi: 10.1061/(asce)ee.1943-7870.0001328.

[15] S. Sharifi, R. Nabizadeh, B. Akbarpour, A. Azari, H.R. Ghaffari, S. Nazmara, B. Mahmoudi, L. Shiri, M. Yousefi, Modeling and optimizing parameters affecting hexavalent chromium adsorption from aqueous solutions using Ti-XAD7 nanocomposite: RSM-CCD approach, kinetic, and isotherm studies, J. Environ. Health Sci. Eng., 17 (2019) 873–888.

[16] S.J.S. Chelladurai, K. Murugan, A.P. Ray, M. Upadhyaya, V. Narasimharaj, S. Gnanasekaran, Optimization of process

parameters using response surface methodology: a review, Mater. Today:. Proc., 37 (2020) 1301–1304.

[17] M.P. Gomes, J.C.M. de Brito, M.M.L. Carvalho Carneiro, M.R. Ribeiro da Cunha, Q.S. Garcia, C.C. Figueredo, Responses of the nitrogen-fixing aquatic fern Azolla to water contaminated with ciprofloxacin: impacts on biofertilization, Environ. Pollut., 232 (2018) 293–299.

[18] A.R. Mahmood, H.H. Al-Haideri, F.M. Hassan, Detection of antibiotics in drinking water treatment plants in Baghdad City, Iraq, Adv. Public Health, 2019 (2019) 1–10, doi: 10.1155/2019/7851354.

[19] Y. Tang, Q. Chen, W. Li, X. Xie, W. Zhang, X. Zhang, H. Chai, Y. Huang, Engineering magnetic N-doped porous carbon with super-high ciprofloxacin adsorption capacity and wide pH adaptability, J. Hazard. Mater., 388 (2020) 122059, doi: 10.1016/j.jhazmat.2020.122059.

[20] S. Sivaselvam, P. Premasudha, C. Viswanathan, N. Ponpandian, Enhanced removal of emerging pharmaceutical contaminant ciprofloxacin and pathogen inactivation using morphologically tuned MgO nanostructures, J. Environ. Chem. Eng., 8 (2020) 104256, doi: 10.1016/j.jece.2020.104256.

[21] E.C. Ngeno, V.O. Shikuku, F. Orata, L.D. Baraza, S.J. Kimosop, Caffeine and ciprofloxacin adsorption from water onto clinoptilolite: linear isotherms, kinetics, thermodynamic and mechanistic studies, S. Afr. J. Chem., 72 (2019) 136–142.

[22] A. Avcı, İ. İnci, N. Baylan, Adsorption of ciprofloxacin hydrochloride on multiwall carbon nanotube, J. Mol. Struct., 1206 (2020) 1–7, doi: 10.1016/j.molstruc.2020.127711.

[23] A. Avcı, İ. İnci, N. Baylan, A comparative adsorption study with various adsorbents for the removal of ciprofloxacin hydrochloride from water, Water Air Soil Pollut., 230 (2019), doi: 10.1007/s11270-019-4315-6.

[24] S. Yi, B. Gao, Y. Sun, J. Wu, X. Shi, B. Wu, X. Hu, Removal of levofloxacin from aqueous solution using rice-husk and wood-chip biochars, Chemosphere, 150 (2016) 694–701.

[25] T.D. Pham, T.T. Bui, V.T. Nguyen, T.K.V. Bui, T.T. Tran, Q.C. Phan, T.D. Pham, T.H. Hoang, Adsorption of polyelectrolyte onto nanosilica synthesized from rice husk: characteristics, mechanisms, and application for antibiotic removal, Polymers (Basel), 10 (2018), doi: 10.3390/polym10020220.

[26] Y. Chen, F. Wang, L. Duan, H. Yang, J. Gao, Tetracycline adsorption onto rice husk ash, an agricultural waste: its kinetic and thermodynamic studies, J. Mol. Liq., 222 (2016) 487–494.

[27] Y.-T. Huang, L.-C. Lee, M.-C. Shih, W.-T. Huang, Introductory of Excel Spreadsheet for comparative analysis of linearized expressions of Langmuir isotherm for methylene blue onto rice husk, Int. J. Sci. Res. Publ., 9 (2019) 8587, doi: 10.29322/ijsrp.9.01.2019.p8587.

[28] A. Ahmad, N. Khan, B.S. Giri, P. Chowdhary, P. Chaturvedi, Removal of methylene blue dye using rice husk, cow dung and sludge biochar: characterization, application, and kinetic studies, Bioresour. Technol., 306 (2020) 123202, doi: 10.1016/j.biortech.2020.123202.

[29] S.K. Hubadillah, M.H.D. Othman, Z. Harun, A.F. Ismail, M.A. Rahman, J. Jaafar, A novel green ceramic hollow fiber membrane (CHFM) derived from rice husk ash as combined adsorbent-separator for efficient heavy metals removal, Ceram. Int., 43 (2017) 4716–4720.

[30] J. Shi, X. Fan, D.C.W. Tsang, F. Wang, Z. Shen, D. Hou, D.S. Alessi, Removal of lead by rice husk biochars produced at different temperatures and implications for their environmental utilizations, Chemosphere, 235 (2019) 825–831.

[31] M.C. Hoyos-Sánchez, A.C. Córdoba-Pacheco, L.F. Rodríguez-Herrera, R. Uribe-Kaffure, Removal of Cd(II) from aqueous media by adsorption onto chemically and thermally treated rice husk, J. Chem., 2017 (2017), doi: 10.1155/2017/5763832.

[32] A. Petersons, Skin and Soft Tissues, Pediatr. Surg. Dig., 2009, pp. 711–719, doi: 10.1007/978-3-540-34033-1_36.

[33] M.J. M-Ridha, S.I. Hussein, Z.T. Alismaeel, M.A. Atiya, G.M. Aziz, Biodegradation of reactive dyes by some bacteria using response surface methodology as an optimization technique, Alexandria Eng. J., 59 (2020) 3551–3563.

[34] A. Asfaram, M. Ghaedi, S. Agarwal, I. Tyagi, V.K. Gupta, Removal of basic dye Auramine-O by ZnS:Cu nanoparticles loaded on activated carbon: optimization of parameters using response surface methodology with central composite design, RSC Adv., 5 (2015) 18438–18450.

[35] P. Sutradhar, P. Maity, S. Kar, S. Poddar, Modelling and optimization of PSA (pressure swing adsorption) unit by using aspen Plus® and design expert ®, Int. J. Innov. Technol. Explor. Eng., 8 (2019) 64–69.

[36] A. Prof, S. Esmail, S.Y. Mohammed, Removal of cadmium ions from simulated wastewater using rice husk biosorbent, J. Eng., 18 (2012) 868–875.

[37] U. Khalil, M. Bilal Shakoor, S. Ali, M. Rizwan, M. Nasser Alyemeni, L. Wijaya, Adsorption-reduction performance of tea waste and rice husk biochars for Cr(VI) elimination from wastewater, J. Saudi Chem. Soc., 24 (2020) 799–810.

[38] S. Álvarez-Torrellas, A. Rodríguez, G. Ovejero, J. García, Comparative adsorption performance of ibuprofen and tetracycline from aqueous solution by carbonaceous materials, Chem. Eng. J., 283 (2016) 936–947.

[39] U.J. Ahile, H.N. Iorav, L. Dooga, D. Terungwa, S.D. Igbawase, K. Asemawe, S.T. Torsabo, Preparation, characterization and application of rice husk adsorbent in the removal of ampicillin from aqueous solution, Int. J. Mod. Chem., 11 (2019) 28–39.

[40] A. Fakhri, Application of response surface methodology to optimize the process variables for fluoride ion removal using maghemite nanoparticles, J. Saudi Chem. Soc., 18 (2014) 340–347.

[41] M. Sedighi, S.A. Aljlil, M.D. Alsubei, M. Ghasemi, M. Mohammadi, Performance optimisation of microbial fuel cell for wastewater treatment and sustainable clean energy generation using response surface methodology, Alexandria Eng. J., 57 (2018) 4243–4253.

[42] L.M. S. Pereira, T.M. Milan, D.R. Tapia-Blácido, Using response surface methodology (RSM) to optimize 2G bioethanol production: a review, Biomass Bioenergy, 151 (2021), doi: 10.1016/j.biombioe.2021.106166.

[43] D.M. Barends, M.E. Olivera, R.H. Manzo, H.E. Junginger, K.K. Midha, V.P. Shah, S. Stavchansky, J.B. Dressman, Delivery of the photosensitizer Pc 4 in PEG–PCL micelles for in vitro PDT studies, J. Pharm. Sci., 99 (2010) 2386–2398.

[44] U.E. Osonwa, J.I. Ugochukwu, E.E. Ajaegbu, K.I. Chukwu, R.B. Azevedo, C.O. Esimone, Enhancement of antibacterial activity of ciprofloxacin hydrochloride by complexation with sodium cholate, Bull. Fac. Pharm., Cairo Univ., 55 (2017) 233–237.

[45] P. Liu, W.J. Liu, H. Jiang, J.J. Chen, W.W. Li, H.Q. Yu, Modification of bio-char derived from fast pyrolysis of biomass and its application in removal of tetracycline from aqueous solution, Bioresour. Technol., 121 (2012) 235–240.

[46] M.E. Mahmoud, A.M. El-Ghanam, R.H.A. Mohamed, S.R. Saad, Enhanced adsorption of Levofloxacin and Ceftriaxone antibiotics from water by assembled composite of nanotitanium oxide/chitosan/nano-bentonite, Mater. Sci. Eng. C, 108 (2020) 110199, doi: 10.1016/j.msec.2019.110199.

[47] Y. Xiang, Z. Xu, Y. Zhou, Y. Wei, X. Long, Y. He, D. Zhi, J. Yang, L. Luo, A sustainable ferromanganese biochar adsorbent for effective levofloxacin removal from aqueous medium, Chemosphere, 237 (2019) 124464, doi: 10.1016/j.chemosphere.2019.124464.

[48] F. Wang, B. Yang, H. Wang, Q. Song, F. Tan, Y. Cao, Removal of ciprofloxacin from aqueous solution by a magnetic chitosan grafted graphene oxide composite, J. Mol. Liq., 222 (2016) 188–194.

[49] E.S.I. El-Shafey, H. Al-Lawati, A.S. Al-Sumri, Ciprofloxacin adsorption from aqueous solution onto chemically prepared carbon from date palm leaflets, J. Environ. Sci. (China), 24 (2012) 1579–1586.

[50] M.R. Majeed, A.S. Muhammed, K.A. Rasheed, The removal of zinc, chromium and nickel from industrial waste water using rice husk, Iraqi J. Sci., 55 (2014) 411–418.

[51] M.E. Peñafiel, E. Vanegas, D. Bermejo, J.M. Matesanz, M.P. Ormad, Organic residues as adsorbent for the removal

of ciprofloxacin from aqueous solution, Hyperfine Interact., 240 (2019), doi: 10.1007/s10751-019-1612-9.

[52] T.D. Pham, T.N. Vu, H.L. Nguyen, P.H.P. Le, T.S. Hoang, Adsorptive removal of antibiotic ciprofloxacin from aqueous solution using protein-modified nanosilica, Polymers (Basel), 12 (2020), doi: 10.3390/polym12010057.

[53] R.M. Ali, H.A. Hamad, M.M. Hussein, G.F. Malash, Potential of using green adsorbent of heavy metal removal from aqueous solutions: adsorption kinetics, isotherm, thermodynamic, mechanism and economic analysis, Ecol. Eng., 91 (2016) 317–332.

[54] V. Srivastava, Y.C. Sharma, M. Sillanpää, Green synthesis of magnesium oxide nanoflower and its application for the removal of divalent metallic species from synthetic wastewater, Ceram. Int., 41 (2015) 6702–6709.

[55] U. Guyo, T. Makawa, M. Moyo, T. Nharingo, B.C. Nyamunda, T. Mugadza, Application of response surface methodology for Cd(II) adsorption on maize tassel-magnetite nanohybrid adsorbent, J. Environ. Chem. Eng., 3 (2015) 2472–2483.

[56] Z.N. Garba, N.I. Ugbaga, A.K. Abdullahi, Evaluation of optimum adsorption conditions for Ni(II) and Cd(II) removal from aqueous solution by modified plantain peels (MPP), Beni-Suef Univ. J. Basic Appl. Sci., 5 (2016) 170–179.

[57] A.A. Inyinbor, F.A. Adekola, G.A. Olatunji, Kinetics, isotherms and thermodynamic modeling of liquid phase adsorption of Rhodamine B dye onto Raphia hookerie fruit epicarp, Water Resour. Ind., 15 (2016), doi: 10.1016/j.wri.2016.06.001.

[58] R. Li, Z. Wang, J. Guo, Y. Li, H. Zhang, J. Zhu, X. Xie, Enhanced adsorption of ciprofloxacin by KOH modified biochar derived from potato stems and leaves, Water Sci. Technol., 77 (2018) 1127–1136.

[59] S. Wu, Y. Li, X. Zhao, Q. Du, Z. Wang, Y. Xia, L. Xia, Biosorption behavior of ciprofloxacin onto *Enteromorpha prolifera*: isotherm and kinetic studies, Int. J. Phytorem., 17 (2015) 957–961.

[60] L. Wang, C. Yang, A. Lu, S. Liu, Y. Pei, X. Luo, An easy and unique design strategy for insoluble humic acid/cellulose nano-composite beads with highly enhanced adsorption performance of low concentration ciprofloxacin in water, Bioresour. Technol., 302 (2020), doi: 10.1016/j.biortech.2020.122812.

[61] E.C. Ngeno, F. Orata, L.D. Baraza, V.O. Shikuku, S.J. Kimosop, Adsorption of caffeine and ciprofloxacin onto pyrolitically derived water hyacinth biochar: isothermal, kinetic and thermo-dynamic studies, J. Chem. Chem. Eng., 10 (2016) 185–194.

[62] N. Dhiman, N. Sharma, Removal of pharmaceutical drugs from binary mixtures by use of ZnO nanoparticles: (competitive adsorption of drugs), Environ. Technol. Innovation, 15 (2019) 100392, doi: 10.1016/j.eti.2019.100392.

[63] H. Rashidi Nodeh, H. Sereshti, Synthesis of magnetic graphene oxide doped with strontium titanium trioxide nanoparticles as a nanocomposite for the removal of antibiotics from aqueous media, RSC Adv., 6 (2016) 89953–89965.

[64] M. Naushad, S. Vasudevan, G. Sharma, A. Kumar, Z.A. Alothman, Adsorption kinetics, isotherms, and thermo-dynamic studies for Hg^{2+} adsorption from aqueous medium using alizarin red-S-loaded amberlite IRA-400 resin, Desal. Water Treat., 57 (2016) 18551–18559.